KTa0.6Nb0.4O3 Ferroelectric Thin Film Behavior at Microwave Frequencies for Tunable Applications

Vincent Laur, Anthony Rousseau, Gérard Tanné, Paul Laurent, Stéphanie Députier, Maryline Guilloux-Viry, Fabrice Huret

$KTa_{0.6}Nb_{0.4}O_3$ Ferroelectric Thin Film Behavior at Microwave Frequencies for Tunable Applications

Vincent Laur, Anthony Rousseau, Gérard Tanné, *Member, IEEE*, Paul Laurent, *Member, IEEE*, Stéphanie Députier, Maryline Guilloux-Viry, and Fabrice Huret, *Member, IEEE*

***Abstract*—In this study about the relationships between structural and microwave electrical properties of $KTa_{1\text{-}x}Nb_xO_3$ (KTN) ferroelectric materials, a KTN thin film was deposited on different substrates to investigate how KTN growth affects the microwave behavior. Interdigital capacitors and stubs were made on these films through a simple engraving process. Microwave measurements under a static electric field showed the importance of the substrate on the circuit behavior and, notably, on the tuning factor.**

I. Introduction

Telecommunication systems are continually evolving because technical improvements have opened several opportunities in wireless communications such as telephones, data transmission, or television. This phenomenon has increased the number of standards associated with these new technologies. Over the last decade, laboratories have studied agile devices that might provide solutions for system miniaturization, which is slowed down by the emergence of new services. Ferromagnetic materials and microelectromechanical systems have shown interesting performances in this way. A collaboration between our laboratory (LEST) and that of Unité Sciences Chimiques-Rennes (USC) has been started in order to investigate the integration of ferroelectric materials into microwave functions so as to achieve agile devices for front-end radio at room temperature. Indeed, both the permittivity of ferroelectrics and dielectric losses can be changed by applying an electric field. In planar technology, bias voltage is easy to integrate and leads to few additional losses. Most of the research about these materials deals with $Ba_{1\text{-}x}Sr_xTiO_3$ (BST) ferroelectrics [1], [2]. These materials have demonstrated agility properties of high interest for microwave frequencies.

The investigations reported here were focused on $KTa_{0.6}Nb_{0.4}O_3$ (KTN) materials, which have, like BST, a crystal structure of the perovskite type [3]. Their Curie temperature (T_c) can be modified by adjusting the tantalum-to-niobium ratio in the final compound. For bulk material, the law governing the T_c value is: $T_c(x) = 676x + 32$ (K), where x is the proportion of niobium [4]. It is worth recalling that, in thin film, the value of T_c can be modified by changing the shape factor or the strains in the film. Our study is focused on the $KTa_{0.6}Nb_{0.4}O_3$ composition; its T_c in bulk material is 302 K, which is close to 293 K (room temperature). The study of its microwave properties on four different growth substrates will give us information about the effect of the ferroelectric thin-film microstructure on its behavior at high frequencies.

II. Thin Film Preparation

KTN thin films are currently deposited in the USC laboratory by a pulsed laser deposition process. Besides the extensive works published on BST thin films for microwave applications, some groups reported in this field on the growth of KTN films [5] and also on the growth of related compounds such as $Na_{0.5}K_{0.5}NbO_3$ [6]. Difficulties of composition control due to potassium volatility are currently reported [5].

Stoichiometric single-phase films can be achieved provided that deposition parameters are accurately optimized [7].

In this study, KTN thin films were grown *in situ* by pulsed laser deposition with a KrF excimer laser operating at 2 Hz (20-ns pulses, $\lambda = 248$ nm, focused energy density of $\sim$1.5 J/cm^2). The laser beam was focused on the target which was rotated within a standard vacuum chamber (background pressure of about 5.10^{-6} mbar).

KTN thin films were deposited from homemade sintered targets enriched in potassium from KNO_3 to compensate for the potassium lost during deposition. KTN targets were prepared by solid-state reaction through a conventional sintering process. First, the $KTaO_3$ and $KNbO_3$ powders were synthesized from stoichiometric mixtures of, respectively, $K_2CO_3 \cdot 1.5\ H_2O$ and Ta_2O_5, and $K_2CO_3 \cdot 1.5\ H_2O$ and Nb_2O_5, calcined in air at 1000°C for 12 h. Then, cylindrical pellets, 25 mm in diameter, $\sim$5 mm thick, were obtained by sintering $KNbO_3$ and $KTaO_3$ with an excess of potassium as KNO_3 at 350°C for 12 h. The density of the resulting target was in the range of 65–75% of KTN theoretical density; its surface was polished before each deposition run. The thin films were grown at 700°C and 0.3 mbar

Manuscript received July 28, 2005; accepted May 11, 2006.

V. Laur, G. Tanné, P. Laurent, and F. Huret are with LEST-UBO/ENSTBr, UMR CNRS 6165, 29238 Brest Cedex3, France (e-mail: vincent.laur@univ-brest.fr).

A. Rousseau and M. Guilloux-Viry are with Unité Sciences Chimiques de Rennes, UMR 6226 CNRS/Université de Rennes 1, 35042 Rennes, France.

Digital Object Identifier 10.1109/TUFFC.2006.174

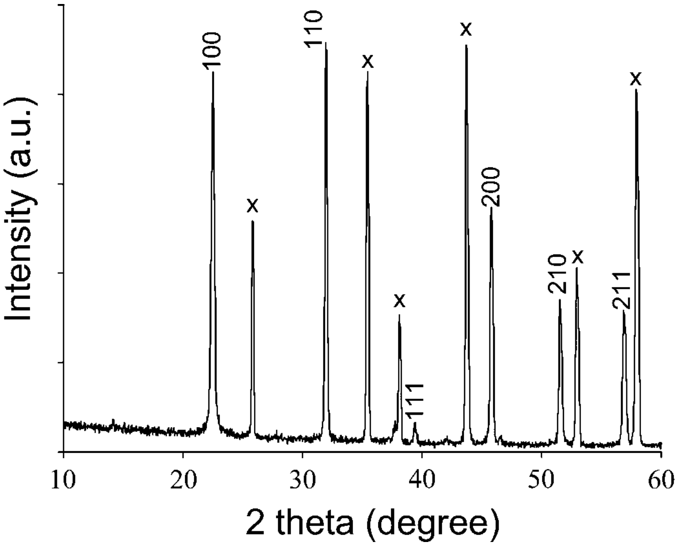

Fig. 1. XRD diagram of a KTN/Al_2O_3 heterostructure. Peaks noted "x" correspond to alumina.

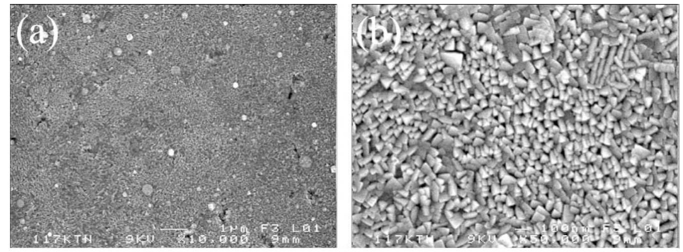

Fig. 2. SEM observation of a thin film of KTN grown on alumina (enlargement × 10000 (a) and × 50000 (b)).

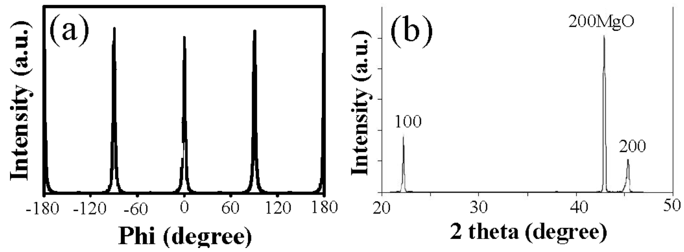

Fig. 3. XRD patterns (a) in φ-scan mode performed on (110) reflection of KTN and (b) in θ-2θ mode of a KTN/MgO heterostructure.

in oxygen pressure and deposited on the substrate placed at about 60 mm from the target in order to produce homogeneous films. Thus, 600-nm-thick films were deposited on a 1-cm^2 surface. The selection of substrates, i.e., sintered alumina, MgO, R-plane sapphire, and lanthanum aluminate ((100)$LaAlO_3$), resulted from a compromise between growth quality and microwave properties. Alumina is frequently used in microwave devices because of its low cost in sintered polycrystalline form; its dielectric constant is about 10, and its loss factor is less than 10^{-3}. Its drawbacks are the lack of epitaxial growth of KTN and the surface roughness even after polishing. MgO single crystal is also suitable as substrate for microwave devices ($\varepsilon_r = 9.4$, $\tan\delta = 9.10^{-3}$). Sapphire consists of a single crystal of alumina; its dielectric properties are very close to those of sintered alumina, with an anisotropy issued from its oriented structure. Finally, the lattice parameters of $LaAlO_3$ being close to those of KTN enable an epitaxial growth together with reasonable dielectric properties ($\varepsilon_r = 24.5$, $\tan\delta = 6.10^{-5}$).

III. Physical and Structural Characterization

The structure of KTN thin films was detailed in [8]. The characterization of films grown on different substrates by x-ray diffraction (XRD) and the microscopic observation of their surface morphology by field effect emission scanning electron microscope operated at low voltage were both performed in the USC laboratory.

The first KTN thin films were grown on sintered alumina under the above-mentioned conditions. The XRD diagram (Fig. 1) shows that alumina favors the growth of a non-oriented structure.

This disordered structure was confirmed by scanning electron microscopy (SEM). Fig. 2 shows a dense microstructure made of grains of very different orientations and shapes; their sizes range from 100 to 150 nm.

The XRD φ-scan diagram of the KTN film on (100)MgO substrate [Fig. 3(a)] was performed with a 4-circle texture diffractometer on the $110_{\mathrm{pseudocubic}}$ reflection ($2\theta \sim 31.6°$, $\chi \sim 45°$); in conjunction with the θ-2θ XRD patterns [Fig. 3(b)], the epitaxial growth of (100)-oriented KTN film is shown.

KTN thin films on LAO also presented a better epitaxial growth than on MgO. This oriented growth led to a dense microstructure made of regular, ordered, and square-shaped grains of size between 50 and 100 nm [Fig. 4(a)]; the surface roughness is, thus, decreased with respect to that of MgO. An XRD analysis of the KTN films on R-plane sapphire showed secondary orientations coexisting with the preferential (100) one, which corresponds to a texture with privileged in-plane orientations, in contrast with an actual epitaxy. The microstructure observed by SEM [Fig. 4(b)] is in agreement with this texture. The grains have sizes similar to those of KTN on LAO.

In conclusion, the noticeable differences observed between the microstructures obtained were dependent on the substrate chosen for thin film growth. By demonstrating the dense and ordered microstructure on LAO sub-

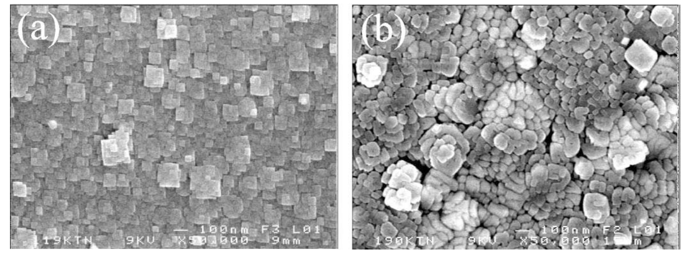

Fig. 4. SEM micrography of KTN/LAO (a) and KTN/sapphire (b) heterostructures.

strate, structural analyses proved the very high quality of its growth. This type of microstructure should produce less dielectric loss than a disordered one, such as on alumina substrates.

IV. Circuit Design and Fabrication

A. Simulation and Design

The first structures fabricated were very basic to permit a reliable assessment of the measured parameters. They consisted of interdigital capacitors and stubs. To achieve our circuits, we used coplanar technology because, compared to the microstrip one, it enhances the interactions between the ferroelectric thin film and the microwave field. Moreover, it allows one to get the same impedance with different slot and feed line widths. Thus, as the variation of permittivity is proportional to the amplitude of the field applied to the material, the designer can select a wide or narrow range of variations.

Simulations of such heterostructures are very difficult with commercial simulators because they tend to split the ferroelectric film into a network of very numerous meshes, at the expense of simulation times.

We calculated the dimensions of our circuits from a combination of electromagnetic and circuit simulations whose principle is illustrated in Fig. 5. The devices under study are first broken down into different parts. Then, the effective permittivity and the characteristic impedance of each part governed by the geometrical dimensions of the line are determined by a spectral domain analysis (SDA). The LineCalc software contained in the circuit simulator advanced design system (ADS) enables us to specify a simple coating substrate with the same effective permittivity as that of the heterostructure of the section of concern. Then, each part is electromagnetically simulated by the Momentum software; this step requires the adjustment of impedances in ports to avoid reflections due to impedance mismatches between the different parts during the final simulation. Last, the results of each independent EM simulation are collected and pooled with the others for the global simulations with ADS.

We thus fabricated interdigital capacitors (IDCs) [Fig. 6(a)] and stubs [Fig. 6(b)] of various dimensions. The finger lengths of IDCs fell within 100 and 400 μm. The gap between fingers and their widths were always 20 μm.

The stub dimensions were such that they allowed evaluation of agility between 3 and 17 GHz. In this band of frequencies, resonance frequencies were determined from changes in the stub lengths. To obtain a high electric field, while taking into account the limitations of our engraving technology, the slots were 20 μm in width.

B. Fabrication

The metallization of circuits and microwave measurements were performed in the LEST. A low-cost engraving

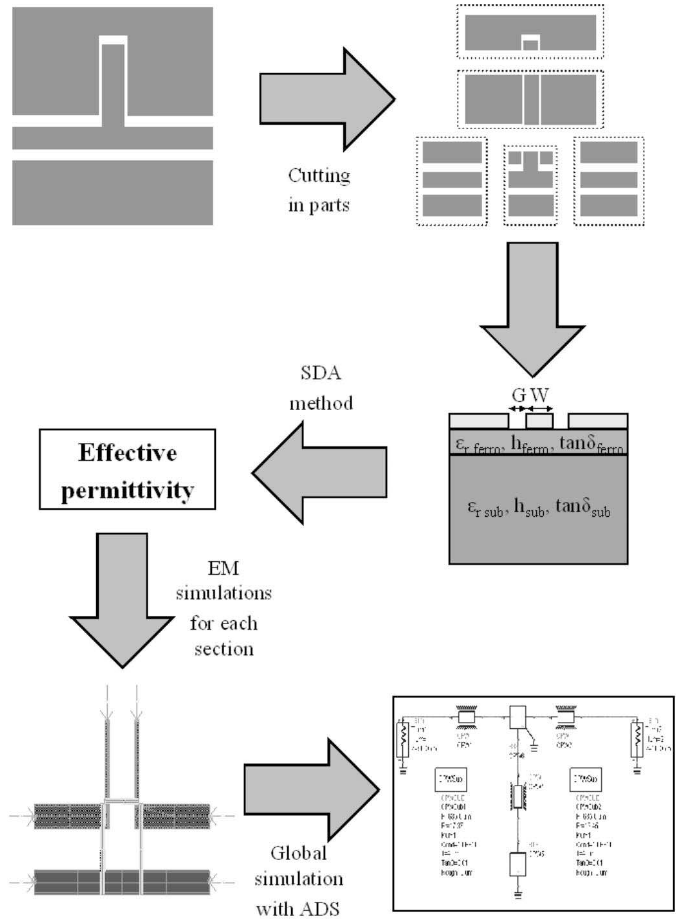

Fig. 5. Block diagram of a stub simulation.

process was used to make the 4-μm-thick gold-plated electrodes.

To avoid cracks in the films caused by a mismatch in thermal dilation coefficients between substrate and ferroelectric material, the firing gold temperature was lowered to 750°C (instead of 800°C). The quality of metallization, which is quite good, was apparently unaffected by this reduction of temperature.

V. Measurements and Analysis

A. Measurement Procedure

As we wondered whether the microstructure of thin films would affect the microwave properties of the $KTa_{0.6}Nb_{0.4}O_3$ ferroelectric material, we measured S-parameters with a 37369A Wiltron vector network analyzer and a probe station. Static electric field was applied to the material via a voltage put directly on the probes. Unfortunately, these electric potentials are limited to a 30-V maximum voltage to avoid damages to the probes by air breakdown. Thus, the maximum amplitude of the electric field available was 15 kV/cm; this value is quite low compared to those found in the literature [9], [10], but, in a first step, it enabled us to evaluate the potential of KTN materials.

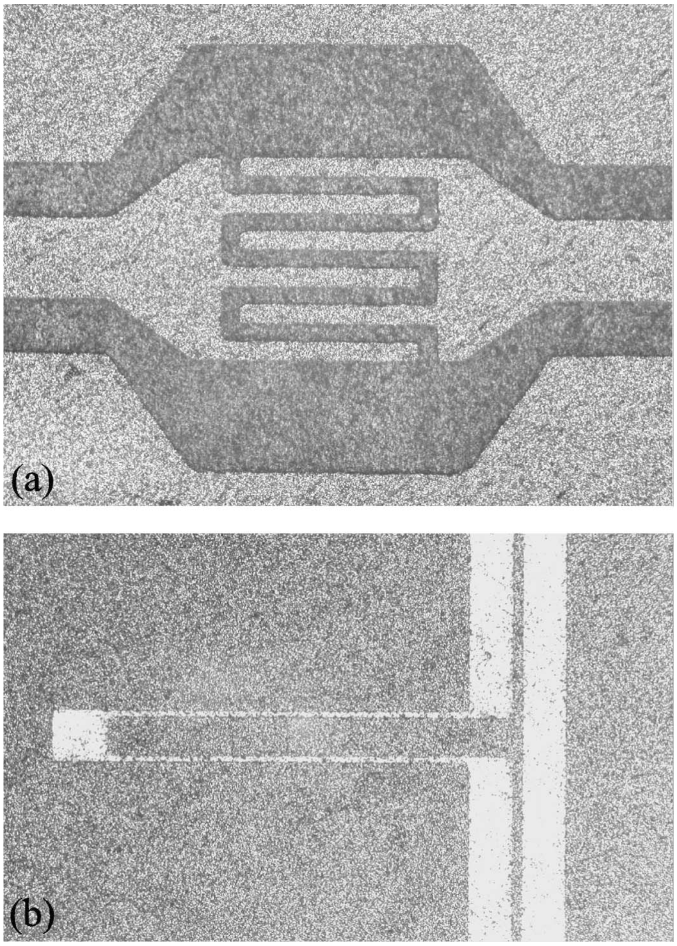

Fig. 6. Micrographs of an interdigital capacitor (a) and a stub (b) in coplanar technology.

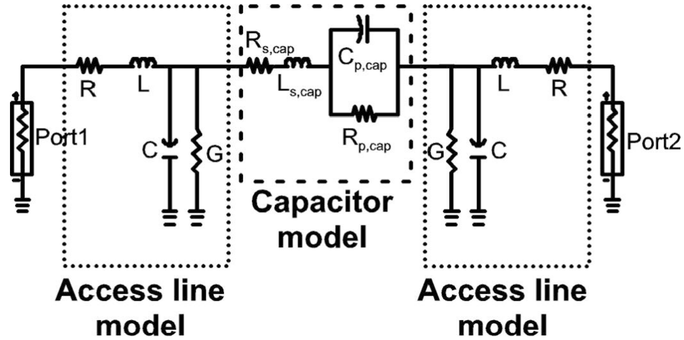

Fig. 7. Global model of the interdigital structure.

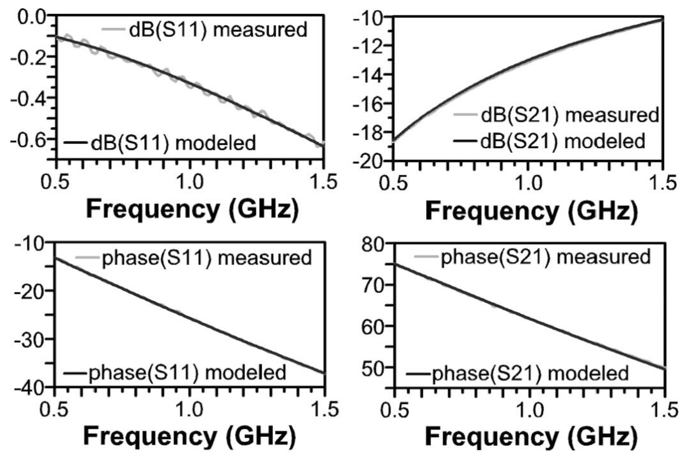

Fig. 8. Comparison of S-parameters between measurement and modeling of an interdigital structure.

The main characteristic studied here is the tuning factor, or agility, issued from the difference between the device responses under a maximum voltage and a null one. As a rule, this tuning factor is defined in (1) where $X = C$ (capacitance) for IDCs and $X = F_r$ (resonance frequency) for a stub. These values are commonly chosen because they are characteristic of such structures; thus they are directly affected by changes in substrate properties.

$$\text{Tuning Factor} = \frac{|X(0V) = X(V_{\max})|}{X(0V)} \tag{1}$$

B. Measurement Analysis

One should note that the determination of resonance frequency is easy for a stub; on the other hand, assessing the effective capacitance of an interdigital structure is more difficult. This led us to use a model proposed by Nash *et al.* [11] for IDCs. However, this model alone failed to take into account the access lines of our structures; we, thus, placed it between the two RLCG circuits equivalent to transmission lines to constitute our global model (Fig. 7).

The values issued from the global model needed adjustment to fit the previously measured IDC S-parameters; this was done with ADS software through an optimization method based on impedances for better accuracy. Fig. 8 illustrates the agreement between modeling and measurement of an IDC fabricated on a $KTa_{0.6}Nb_{0.4}O_3$/sapphire substrate with no voltage applied.

The equivalent capacitance of this IDC is given by the capacitance value issued from the global model. Application of a 30-V maximum voltage to this structure showed that the access lines (in particular, slot widths) are wide enough to avoid effects of the electric field on the ferroelectric material. Changes of permittivity were mainly localized only between the fingers of the interdigital structure where the amplitude is the largest. These observations led us to keep our access lines unchanged in the global model when assessing the variation of capacitance under applied voltage; the only changes made were on the parameters of Nash's model.

C. Measurement Results

IDCs and stubs were fabricated on $KTa_{0.6}Nb_{0.4}O_3$/Al_2O_3, $KTa_{0.6}Nb_{0.4}O_3$/MgO, $KTa_{0.6}Nb_{0.4}O_3$/LAO, and $KTa_{0.6}Nb_{0.4}O_3$/sapphire. S-parameter measurements enabled us to obtain significant values such as a quality factor of the structure, Q, and its agility. Table I sums up the results concerning the microstructure of the ferroelectric

TABLE I
SUBSTRATE AND CIRCUIT PROPERTIES.

	Al_2O_3	MgO	$LaAlO_3$	Sapphire
Structure type	Polycrystal	Monocrystal	Monocrystal	Monocrystal
Dielectric constant	9.9	9.4	24.5	11.5 // c, 9.4 $\perp$ c
Loss tangent	$< 10^{-3}$	9.10^{-3}	6.10^{-5}	3.10^{-6} // c, 9.10^{-6} $\perp$ c
KTN growth	non-oriented	epitaxial (sticking troubles)	epitaxial	textured
IDC agility at 1 GHz (%)	1.3	3.4	4.6	7.2
Q of IDC at 1 GHz	1.7	7.6	10.7	9.6
Stub agility (%)	< 1	< 1	2.2	4.2

films, the substrate properties and the microwave behavior.

1. IDC Measurements: Table I shows that the agility of IDCs is extremely dependent on the substrate growth. Indeed, on alumina, this factor is only 1.3% at 1 GHz and under a 15-kV/cm electric field; this poor agility can be explained by the disordered microstructure of the films. On MgO substrate, the tuning factor is about 4% under the same conditions; it is higher than on alumina mainly because of a better film growth. However, this agility could have been elevated more if some sticking troubles between the substrate and the film had not occurred during the engraving process. LAO showed an extremely good growth and interesting mechanical performance; agility with this substrate was about 4.6%. The best tuning factor, 7.2%, was provided by sapphire despite the textured growth of KTN thin film, supposed to be less efficient than an epitaxial growth. But, compared to sapphire, the high dielectric constant of LAO weakened the effect of any change in ferroelectric permittivity on the equivalent capacitance.

Another interesting characteristic of the IDCs is their quality factor Q, defined in (2), where Z_{in} is extracted from the measured input reflection parameter of the structure; it represents the ratio of stored energy to the average energy dissipated in the loaded structure, and is dependent on the substrate dielectric loss factor, the ferroelectric thin-film loss tangent, and metallic losses.

$$Q = \frac{\mathrm{im}\,(Z_{\mathrm{in}})}{\mathrm{real}\,(Z_{\mathrm{in}})} \tag{2}$$

Fig. 9 shows that this quality factor decreases exponentially with increasing frequencies for all substrates except

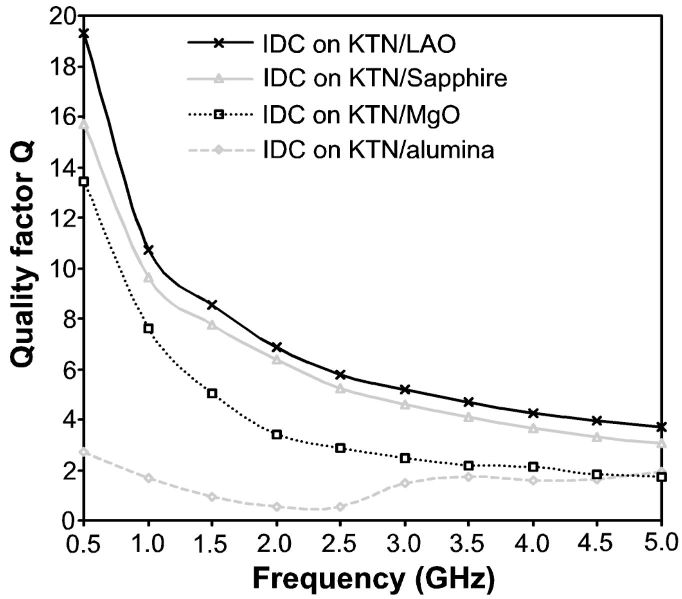

Fig. 9. Quality factor of IDCs as a function of frequency and growth substrate.

alumina. The measured values are poor, but take into account access lines and contacts with probes; so the intrinsic Q factors of the IDCs are actually better than the values reported here. The lowest quality factor was produced by the IDC made on KTN/alumina, likely because of the non-oriented structure in the ferroelectric film at the origin of a high dielectric loss factor. For example, the dielectric loss factor of a film grown on alumina under the same conditions was found to lie between 0.15 and 0.30 [8]. It is worth noting the deterioration of Q by high dielectric losses.

Table I shows that the best Q was provided by KTN/LAO. The MgO one, noticeably poorer, should have been higher if there had been no sticking troubles. The example of sapphire indicates that a textured structure gives a lower Q than an epitaxial structure, because intrinsic sapphire dielectric losses are thought to be lower than LAO ones ($\tan\delta \approx 6.10^{-5}$ for LAO, $\tan\delta < 10^{-5}$ for sapphire).

Fig. 10 illustrates the evolution of normalized Q factors (with respect to its value at 0 V) versus applied voltage for two IDCs made on KTN/sapphire and on KTN/LAO; Q factors were normalized to compare their evolutions. It is obvious that the normalized quality factor on LAO is increased less when a voltage is applied. This observation proves the interest of using a substrate with a moderate permittivity in order to enhance the effects induced by variations of permittivity or losses in the ferroelectric film.

2. Stub Measurements: These four heterostructures were also used to realize stubs in planar technology. Our first measurements made on these stubs showed that the transmission parameters were affected by the numerous resonances induced by the simultaneous propagation of the even and odd modes.

Addition of bridges, especially above tee-junctions, suppressed the propagation of the odd mode and elevated

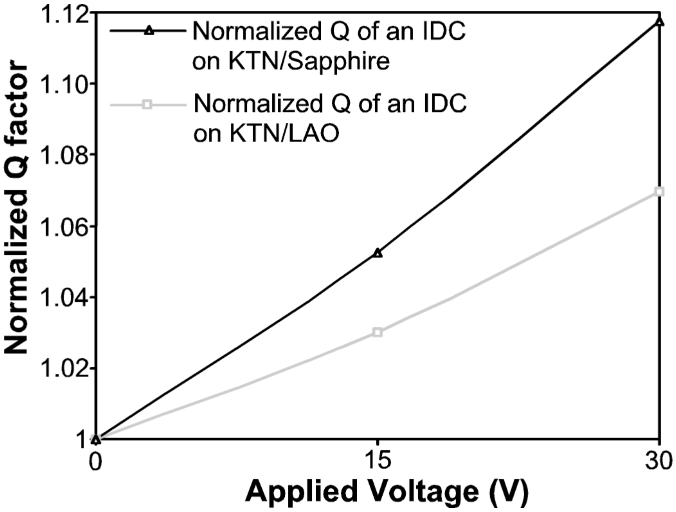

Fig. 10. Evolution of the normalized quality factor of two different IDCs versus applied voltage at 1 GHz.

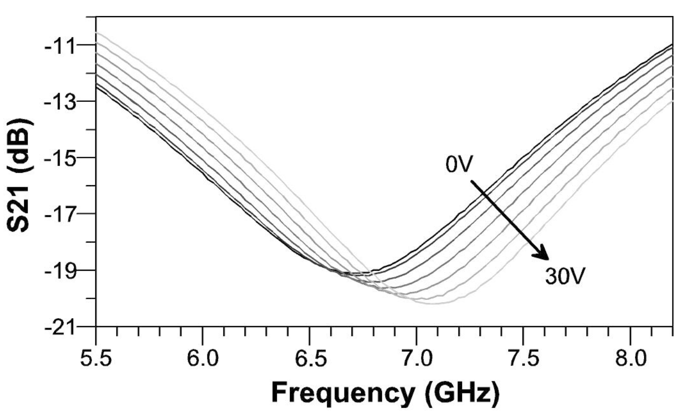

Fig. 11. Transmission parameters of a stub on $KTa_{0.6}Nb_{0.4}O_3$/ sapphire with air-bridges for different applied voltages.

slightly the tuning factor given by (1). Agility on alumina substrate was less than 1% for a resonance frequency around 7 GHz. Comparisons of a given stub made on each of the four substrates highlighted the similarity of performances between alumina and MgO; with LAO, the tuning factor was about 2.2%. Sapphire gave the highest values, 5.0 and 5.6%, without and with bridges, respectively (Fig. 11).

Depending on the voltage applied, 0 and 30 V, the resonance frequency for the $KTa_{0.6}Nb_{0.4}O_3$/sapphire stub was, respectively, 6.70 and 7.08 GHz. The reduction of dielectric losses is indicated by changes in transmission parameters, i.e., improvement of the resonance peak level with increasing voltages.

Stubs and IDCs seem to have a similar behavior. Sapphire, once again, provided the best performances despite its textured structure; it is worth noting that its agility value is promising when considering the low amplitude of the electric field (15 kV/cm) applied to this material. Increasing this electric field should enable us to noticeably enhance agility.

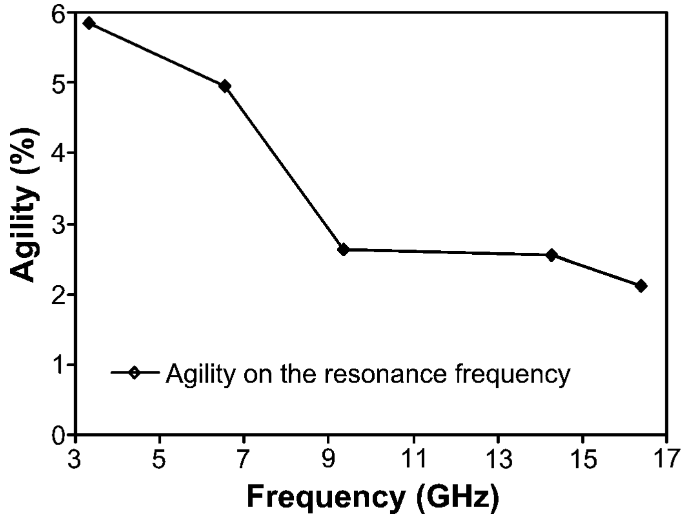

Fig. 12. Agility on the resonance frequency versus frequency. Note that each point corresponds to a different-length stub.

From measurements made on five $KTa_{0.6}Nb_{0.4}O_3$/ sapphire stubs of different lengths, Fig. 12 highlights the decrease of the tuning factor when the frequencies are increased from 3 to 17 GHz. Agility, 6% at about 3 GHz, decreases up to 9 GHz where it becomes nearly stabilized at about 2.5%. This phenomenon can be due to the evolution of the ferroelectric material permittivity against frequency. Dielectric characterizations are in progress and will give us more information.

This study about the possible consequences of KTN thin-film microstructure on microwave properties suggests that both Q factor and agility are dependent on growth quality and substrate dielectric properties.

VI. Conclusion

We reported on the fabrication of agile circuits based on KTN ferroelectric material, from the making of thin films to microwave measurement analyses. The influence of the growth substrate was demonstrated through measurements of identical circuits on different heterostructures. Among them, sapphire demonstrated the best agility because of its moderate permittivity associated with a rather good thin-film growth. LAO substrate produced the best quality of growth, and thus the highest quality factor. In a near future, these substrates will be used to thoroughly investigate the behavior of KTN thin films under high electric field and against temperature.

Acknowledgment

The authors thank R. Jézéquel for spending much time on circuit measurements. We also wish to thank B. Della and G. Chuiton for their user-friendly help in the realization of the circuits. SEM observations were performed at Centre de Microscopie Electronique à Balayage et d'Analyse (Université de Rennes 1).

References

[1] O. G. Vendik, *Ferroelectrics in Microwave Technology.* Moscow: Sov. Radio, 1979.

[2] S. S. Gevorgian and E. L. Kollberg, "Do we really need ferroelectrics in paraelectric phase only in electrically controlled microwave devices," *IEEE Trans. Microwave Theory Tech.*, vol. 49, no. 11, pp. 2117–2124, Nov. 2001.

[3] B. M. Nichols, B. H. Hoerman, J. H. Hwang, T. O. Mason, and B. W. Wessels, "Phase stability of epitaxial $KTa_xNb_{1-x}O_3$ thin films deposited by MOVCD," *J. Mater. Res.*, vol. 18, no. 1, pp. 106–110, Jan. 2003.

[4] D. Rytz and H. J. Scheel, "Crystal growth of $KTa_xNb_{1-x}O_3$ ($0 < x \leq 0.04$) solids solutions by a slow-cooling method," *J. Crystal Growth*, vol. 59, pp. 468–484, 1982.

[5] A. C. Carter, J. S. Horwitz, D. B. Chrisey, J. M. Pond, S. W. Kirchoefer, and W. Chang, "Pulsed laser deposition of ferroelectric thin films for room temperature active microwave electronics," *Integr. Ferroelect.*, vol. 17, pp. 273–285, 1997.

[6] S. Abadei, S. Gevorgian, C. R. Cho, A. Grishin, J. Andreasson, and T. Lindbäck, "DC Field dependent properties of $Na_{0.5}K_{0.5}NbO_3/SiO_2/Si$ structures at millimeter—wave frequencies," *Appl. Phys. Lett.*, vol. 78, pp. 1900–1903, 2001.

[7] A. Rousseau, V. Laur, M. Guilloux-Viry, G. Tanné, P. Laurent, F. Huret, V. Bouquet, and A. Perrin, "Pulsed laser deposited $KNbO_3$ thin films for applications in high frequency range," *Thin Solid Films*, to be published.

[8] A. Rousseau, M. Guilloux-Viry, V. Bouquet, A. Perrin, G. Tanné, F. Huret, J. F. Seaux, D. Cros, and V. Madrangeas, "Ferroelectric thin films for applications in high frequency range," *Ferroelectrics*, vol. 316, pp. 7–12, 2005.

[9] K. B. Kim, T. S. Yun, R. Y. Kim, H. S. Kim, and J. C. Lee, "BST interdigital capacitors with high tunability on MgO substrate," *Microwave Opt. Technol. Lett.*, vol. 45, no. 1, pp. 15–18, Apr. 2005.

[10] W. Chang, S. W. Kirchoefer, J. A. Belletti, and J. M. Pond, "(Ba,Sr)TiO_3 ferroelectric thin films for tunable applications," *Rev. Mex. Fis.*, vol. 50, no. 5, pp. 501–505, Oct. 2004.

[11] J. Nash, D. Ghosh, J. P. Maria, M. B. Steer, A. Kingon, and G. T. Stauf, "Microwave properties of BST thin film interdigital capacitors on low cost alumina substrates," presented at 34th Eur. Microwave Conf., Amsterdam, 2004.

Vincent Laur is currently in his second year of preparation for a Ph.D. degree in electronics from the University of Brest, France. He earned a one-year research-oriented postgraduate degree in telecommunication systems and technologies in 2004. His research interests are focused on agility in microwave using ferroelectric thin films.

Anthony Rousseau received his Ph.D. degree in chemistry from the University of Rennes 1, France, in October 2005. His research interests are focused on ferroelectric thin film growth by pulsed laser deposition and on structural and microstructural thin film characterizations.

Gérard Tanné received his Ph.D. degree in electronics from the University of Brest, Brest, France, in 1994. Since 1995, he has been an Assistant Professor with the Electronic Department, Université de Bretagne Occidentale (UBO), Brest, France. He currently conducts research with the Laboratoire d'Electronique et Systèmes de Télécommunication (LEST). His research activities are in the area of tunable microwave and RF systems. He studies different planar tunable microwave devices (i.e., filters, phase shifters, etc.) applied principally to mobile communication systems.

Paul Laurent received his Ph.D. degree in electronics from the University of Brest, France, in 1994. Since 1997, he has been an assistant Professor in the Technology University Institute—Electronic department of the Université de Bretagne Occidentale (UBO), Brest, France. He is currently conducting research in the Laboratory for Electronics and Communication Systems (LEST). His research activities are in the area of microwave properties of dielectric and magnetic materials. Recently, his research interests are focused on tunable microwave and RF systems. He studies different planar tunable microwave devices using liquid crystal (phase shifters, antennas, filters, etc.). His works on frequency agility potential are extended to the use of ferromagnetic composite or ferroelectric thin films.

Stéphanie Députier received her Ph.D. degree in chemistry from the University of Rennes 1, Rennes, France, in 1992. Since 1994, she has been an Assistant Professor at the Laboratoire de Chimie du Solide et Inorganique Moléculaire at the University of Rennes 1, Rennes, France. Her research activities involve solid state chemistry (especially phase diagrams study) and the field of thin film growth and structural characterization (in particular focused on ferroelectric oxides).

Maryline Guilloux-Viry received her Ph.D. degree in physics from the University of Rennes 1, Rennes, France, in 1991. She is a researcher at the Centre National de la Recherche Scientifique (CNRS) at the Laboratoire de Chimie du Solide et Inorganique Moléculaire at the University of Rennes 1, Rennes, France. Her main research field concerns epitaxial growth (by pulsed laser deposition and sputtering) and characterization of thin films of complex materials (especially superconductors, ferroelectrics).

Fabrice Huret received his Ph.D. degree in electronics from the University of Lille, Villeneuve d'Ascq, France, in 1991. In 1992, he became an Assistant Professor at the Electromagnetic and Circuits Group of the "Institut d'Electronique, de Microélectronique et de Nanotechnologie" (IEMN), University of Lille. In 2000, he joined the University of Bretagne Occidentale as a Professor. He is involved in new substrate materials and their effects on microwave circuits. His research activities also concern the modeling of ULSI interconnects, design and CEM of SOC and SIP, and microwave circuits for new telecommunication systems.